

**4<sup>th</sup> IAA Planetary Defense Conference – PDC 2015**  
**13-17 April 2015, Frascati, Roma, Italy**

**IAA-PDC-15-P-19**  
**SOLAR-SAILING TRAJECTORY DESIGN FOR CLOSE-UP NEA**  
**OBSERVATIONS MISSION**

**Alessandro Piloni<sup>(1)</sup>, Matteo Ceriotti<sup>(2)</sup> and Bernd Dachwald<sup>(3)</sup>**

<sup>(1)</sup>*University of Glasgow, G12 8QQ Glasgow UK,*

<sup>(2)</sup>*University of Glasgow, G12 8QQ Glasgow UK,*

<sup>(3)</sup>*FH Aachen University of Applied Sciences, 52064 Aachen Germany,*

**Abstract**

Near-Earth Asteroids (NEAs) are an extremely valuable resource to study the origin and evolution of the Solar System more in depth. At the same time, they constitute a serious risk for the Earth in the not-so-remote case of an impact. In order to mitigate the hazard of a potential impact with the Earth, several techniques have been studied so far and, for the majority of them, a good knowledge about the chemical and physical composition of the target object is extremely helpful for the success of the mission. A multiple-rendezvous mission with NEAs, with close-up observations, can help the scientific community to improve the overall knowledge about these objects and to support any mitigation strategy. Because of the cost of this kind of mission in terms of  $\Delta v$ , a solar sail spacecraft is proposed in this study, in order to take advantage of the propellantless characteristic of this system. As part of the DLR/ESA Gossamer roadmap, and thus considering the sailcraft based on this technology, the present work is focused on the search of possible sequences of encounters, with priority on Potentially Hazardous Asteroids (PHAs). Because of the huge amount of NEAs, the selection of the candidates for a multiple rendezvous is firstly a combinatorial problem, with more than a billion of possible sequences for only three consecutive encounters. Moreover, an optimization problem should be solved in order to find a feasible solar-sail trajectory for each leg of the sequence. In order to tackle this mixed combinatorial/optimization problem, the strategy used is divided into two main steps: a sequence search by means of heuristic rules and simplified trajectory models, and a subsequent optimization phase. Preliminary results were presented previously by the authors, demonstrating that this kind of mission is promising. In this paper, we aim to find new sequences by introducing a different approach on the sequence search algorithm and by reducing the area-to-mass ratio of the solar sail. A smaller area-to-mass ratio entails either the possibility to carry on more payload or to reduce the sail area, raising the TRL. A grid search over 10 years of launching dates is carried out, resulting in different sequences of objects depending on the departing date. Two sequences are fully studied and optimized. The mission parameters and trajectories of the sequences found are shown and explained.

**Keywords:** *multiple rendezvous, solar sail, mitigation, asteroid*

## 1. Introduction

In the last decades, Near-Earth Asteroids (NEAs) gained importance in the international community, for planetary defense, science and technology purposes. From a technology point of view, NEAs are considered as the first bridge toward a human exploration of Mars [1, 2]. A human mission to these objects, in fact, offers similar challenges as a mission to the red planet (i.e. same deep-space environment and total mission duration similar to an Earth-Mars transit). On the other hand, total mission duration and  $\Delta v$  required (i.e. propellant needed and therefore launching cost) are below those needed for a complete Mars return mission. As reported in [1], however, the asteroid selection for such a mission shall take into account several characteristics (e.g. size, composition, rotation rate, etc.) for the sake of human safety. Based on the observations taken from the Earth, the characterization of NEAs discovered so far often suffers from uncertainties in physical, chemical and orbital properties. Moreover, some NEAs are defined as Potentially Hazardous Asteroids (PHAs) and even for this scenario, accurate property characterization is needed [3]. Sugimoto et al. [4] underlined well this need of knowledge about NEAs properties for deflection purposes. Even if methods exist to deal with NEA composition uncertainties (e.g. Evidence Theory [4]), Sugimoto showed how some deflection methods, those ones that have a great interaction with the target object (e.g. nuclear interceptor or solar sublimation), are more affected to uncertainties on asteroid composition (i.e. porosity, surface materials, precise shape, etc.). Furthermore, not only the chemical and physical composition, but also the rotation of these objects can have an important role in the success of a mission, either a deflection or a sample mission. In the same paper, in fact, it has been pointed out how rotation periods of small asteroids can be determined with an error comparable to the estimated value itself. This can lead to the failure of a deflection mission which uses, for example, a solar sublimation strategy. Several survey and mitigation programs have been settled for the purpose of a better knowledge of NEA characteristics (NEOSShield [5], NEOWISE [6], IAU Minor Planet Center\*, JPL/NASA Near-Earth Object Program<sup>†</sup> and Stardust<sup>‡</sup> are just five examples), but most of them deal with ground-based observations.

A multiple-rendezvous mission with NEAs, with close-up observations, can help the scientific community to improve the overall knowledge about these objects and to support any future mitigation act. Furthermore, a multiple NEA rendezvous mission is preferable to a single-rendezvous mission because of the reduced cost of each observation. This kind of mission, however, is challenging from a mission planning point of view, because of the large amount of objects discovered so far and the huge different sequences of NEAs that can be chosen. This is first of all a combinatorial problem, with a trajectory optimization problem that should be solved for each leg of the multiple rendezvous in order to test the feasibility of the proposed sequence by the propulsion system used.

In this study, a multiple NEA rendezvous mission through solar sailing is analyzed, due to the propellant-less nature of this kind of technology. A multiple-rendezvous mission, in fact, can be very expensive in terms of the total  $\Delta v$  required. As presented in [7], a solar sail can afford missions otherwise very challenging for traditional low-thrust spacecraft.

---

\* <http://www.minorplanetcenter.net/iau/lists/Dangerous.html>, accessed on 06 March 2015.

† <http://neo.jpl.nasa.gov/index.html>, accessed on 06 March 2015.

‡ <http://www.strath.ac.uk/stardust/>, accessed on 06 March 2015.

Starting from the mission requirements addressed by the reference study of Dachwald et al. [8] as part of the DLR/ESA Gossamer Roadmap to solar sailing [9], and from the preliminary results obtained in a previous work by the authors [7], the current work aims firstly to improve the algorithm for the selection of encounters. A priority with respect to PHAs is considered in the sequence search algorithm. Moreover, a solar sail with a lower performance than the one in the reference papers is taken into account in this study. Although the sailcraft studied in those works is already realistic for near-term solar sailing mission, a decrease in the performances required further raises the Technology Readiness Level (TRL).

The paper is organized as follows. In Section 2, a brief overview of the solar sailing fundamentals is given. Sections 3-4 describe the sequence search algorithm and the optimization process used to test the sequences found, respectively. Section 5 describes in detail the problem taken into account. In Section 6 some results of the method described are shown, while in Section 7 conclusions are drawn and future work is outlined.

## 2. Fundamentals of solar sailing

A solar sail is a completely propellant-free thrust system, using only the impinging sunlight to generate thrust. This means that the mission design is not influenced from the maximum amount of fuel that can be carried on. On the other hand, a solar sail shall be a large and lightweight surface, in order to use as much as possible the energy from the sunlight. Furthermore, for a given area-to-mass ratio, the more reflective the sail surface is, the higher is the acceleration produced.

In the ideal case of perfectly reflecting solar sail, in fact, the force produced on the sail surface  $A$  by the solar radiation pressure  $P$  ( $P = 4.56 \mu\text{Pa}$  at the distance of 1 Astronomical Unit (AU) from the Sun) is:

$$\mathbf{f} = 2PA \cos^2 \alpha \hat{\mathbf{N}} \quad (1)$$

where  $\hat{\mathbf{N}}$  is the unit vector normal to the sail plane that is directed away from the Sun. In the orbital reference frame  $\{\hat{\mathbf{r}}, \hat{\boldsymbol{\theta}}, \hat{\mathbf{h}}\}$ ,  $\hat{\mathbf{N}}$  can be expressed by means of the cone angle  $\alpha$  and the clock angle  $\delta$ , so that  $\hat{\mathbf{N}} = [\cos \alpha \quad \sin \alpha \cos \delta \quad \sin \alpha \sin \delta]^T$ .

The acceleration given by a solar sail at the distance  $r$  from the Sun can be expressed as:

$$\mathbf{a} = a_c \left( \frac{r_{\oplus}}{r} \right)^2 \cos^2 \alpha \hat{\mathbf{N}} \quad (2)$$

where  $r_{\oplus} = 1 \text{ AU}$  is the mean Sun-Earth distance. The term  $a_c$  in Eq. (2) is the so-called characteristic acceleration and it represents the acceleration given by the solar sail facing the Sun (i.e.  $\alpha = 0$ ) at the distance of 1 AU.

In Fig. 1, a sketch of the acceleration produced by a solar sail (Eq. (2)) is shown.

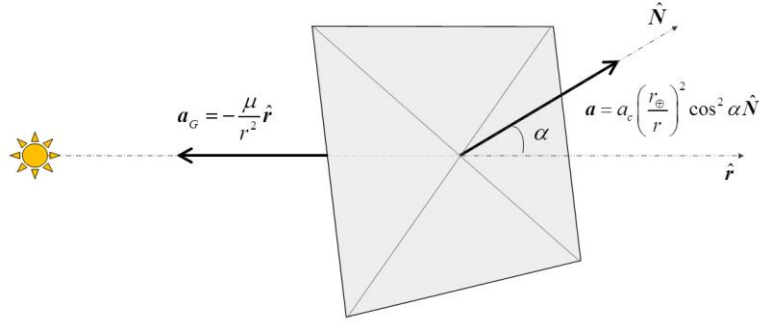


Fig. 1: Sketch of the acceleration produced by a perfectly reflecting solar sail.

By comparing Eq. (1) and Eq. (2) for a sailcraft orbiting at the distance of 1 AU, it can be noticed that the characteristic acceleration can be considered as the solar sail performance index and it depends only by the area-to-mass ratio:

$$a_c = 2P \frac{A}{m} \quad (3)$$

A lower characteristic acceleration means a lower area-to-mass ratio and, therefore, the possibility to use a smaller sail for the same mass of the spacecraft.

### 3. Sequence search

Finding a sequence of NEAs to be visited is first of all a combinatorial problem, because of the large amount of objects and the huge number of possible combinations between those ones, as pointed out in Section 3.1. Furthermore, for each object an optimization problem must be solved in order to test the existence of a solar sail trajectory. For the reasons above, a reduced database of NEAs has been used for the sequence search, as explained in detail in Section 3.1. Moreover, for each leg of the sequence a local pruning on the reduced database has been carried out, in order to reduce further the amount of objects to test, as detailed in Section 3.2.2.

In the following sections, a description of the asteroid selection for the reduced database and a detailed explanation of the sequence search algorithm are given.

#### 3.1. Asteroid database selection

The selection of asteroids to be visited by a spacecraft is difficult to determine, because it shall consider composition, scientific interest, orbital dynamics and available launch windows. There are 11,624 NEAs discovered to date<sup>§</sup> and this number is continuously increasing. All those objects with an Earth Minimum Orbit Intersection Distance (EMOID)  $\leq 0.05$  AU and an absolute magnitude  $H \leq 22$  mag (i.e. diameter  $\geq 110-240$  m, depending on the albedo<sup>\*\*</sup>) are classified as PHAs. Because there are no clear scientific priorities on the selection of NEAs, the problem of finding a sequence of encounters is first of all a combinatorial problem, with more than a billion of possible combinations with permutations of only 3 objects. In order to reduce this huge amount of possible combinations, a second classification method can be considered, taking into account those objects that are part of the Near-Earth

<sup>§</sup> As obtained on 12 November 2014 from NASA's Near-Earth Object Program website ([http://neo.jpl.nasa.gov/cgi-bin/neo\\_elem](http://neo.jpl.nasa.gov/cgi-bin/neo_elem)).  
<sup>\*\*</sup> <http://www.minorplanetcenter.net/iau/lists/Sizes.html>, accessed on 06 March 2015.

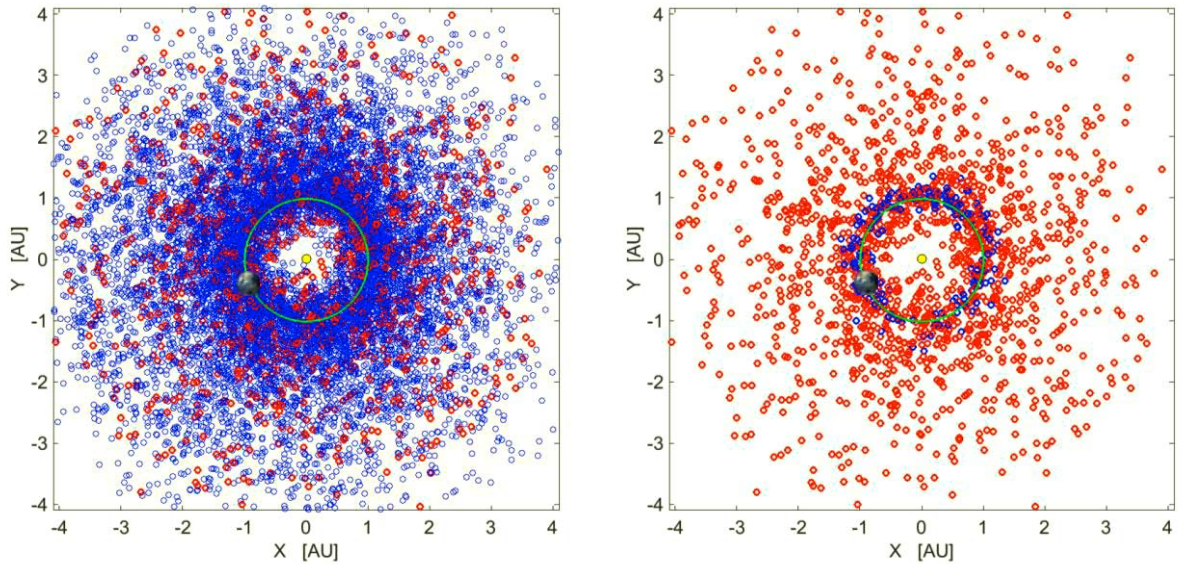
Object Human Space Flight Accessible Target Study (NHATS)<sup>††</sup>. The objects in this list are those ones for whom a low-thrust return mission can be found within the following mission parameters: total  $\Delta v$  required, total mission duration, stay time at the object, launch date interval. Because the mission parameters for the trajectory computation can be set in several different ways, the list of NHATS asteroids is not univocally defined.

In order to have a more usable and interesting database, only PHAs and NHATS asteroids are taken into account in the current work, leading to a reduced database made up of 1,688 objects, 1,514 of which are PHAs. The criteria used to select the NHATS database are the following:

$$\text{NHATS criteria: } \left\{ \begin{array}{l} \text{total } \Delta v \text{ required} \leq 8 \text{ km/s} \\ \text{total mission duration} \leq 450 \text{ days} \\ \text{stay time at the object} \geq 8 \text{ days} \\ \text{launch : 2015 – 2040} \\ H \leq 26 \text{ mag} \\ OCC \leq 7 \end{array} \right. \quad (4)$$

where *OCC* is the Orbit Condition Code of a NEA's orbit, which refers to the accuracy of the orbit determination. For a complete explanation of the above criteria, the interested reader can refer to the JPL/NASA NHATS website.

A graphical comparison between the two databases is given in Fig. 2, where the heliocentric positions of all objects are plotted for both databases, at a given reference time.



a) b)  
Fig. 2: Heliocentric view of the positions of all known NEAs (blue) and PHA (red) on 13<sup>th</sup> April 2015. The whole database (Fig. a) and the modified one (Fig. b) are shown.

<sup>††</sup> <http://neo.jpl.nasa.gov/nhats/>, accessed on 18 November 2014.

An order of magnitude for the problem of finding a sequence of encounters can be given by considering the total number of possible sequences of  $k = 3, 4$  and  $5$  objects without repetition, both from the original and the reduced database. The number of these  $k$ -permutations of  $n$  objects  $P_k^n$  (Table 1) is given by the following:

$$P_k^n = \frac{n!}{(n-k)!} \quad (5)$$

		$k = 3$	$k = 4$	$k = 5$
Complete database	$n = 11,624$	$1.6 \times 10^{12}$	$1.8 \times 10^{16}$	$2.1 \times 10^{20}$
Reduced database	$n = 1,688$	$4.8 \times 10^9$	$8.1 \times 10^{12}$	$1.4 \times 10^{16}$

Table 1: Number of  $k$ -permutations of  $n$  objects within the complete database and the reduced one.

### 3.2. Sequence search algorithm

The sequence search algorithm works as follows (Fig. 3). The whole database used is locally pruned by means of astrodynamical criteria (details in Section 3.2.2) and taking into account that the sequence starts from the Earth at a certain prefixed time  $t_0$ . This pruning allows the algorithm to take into account fewer objects at a time, avoiding spending time on those objects that can be difficult to reach. Approximated solar sail trajectories are adopted, by means of the shape-based approach described in [7] and briefly discussed later (Section 3.2.1). For all the trajectories found, the arrival NEAs are kept and considered as starting object of the next iteration of the algorithm. Next, once the objects in the current pruned list have been tested, the same process is carried out, in a tree search algorithm, starting from the arrival body of each of the temporary sequences found so far. When the total mission duration reaches the maximum allowed time (i.e. 10 years, in the current work) or no feasible solar sail trajectories are found, the loop stops and the sequence found is complete.

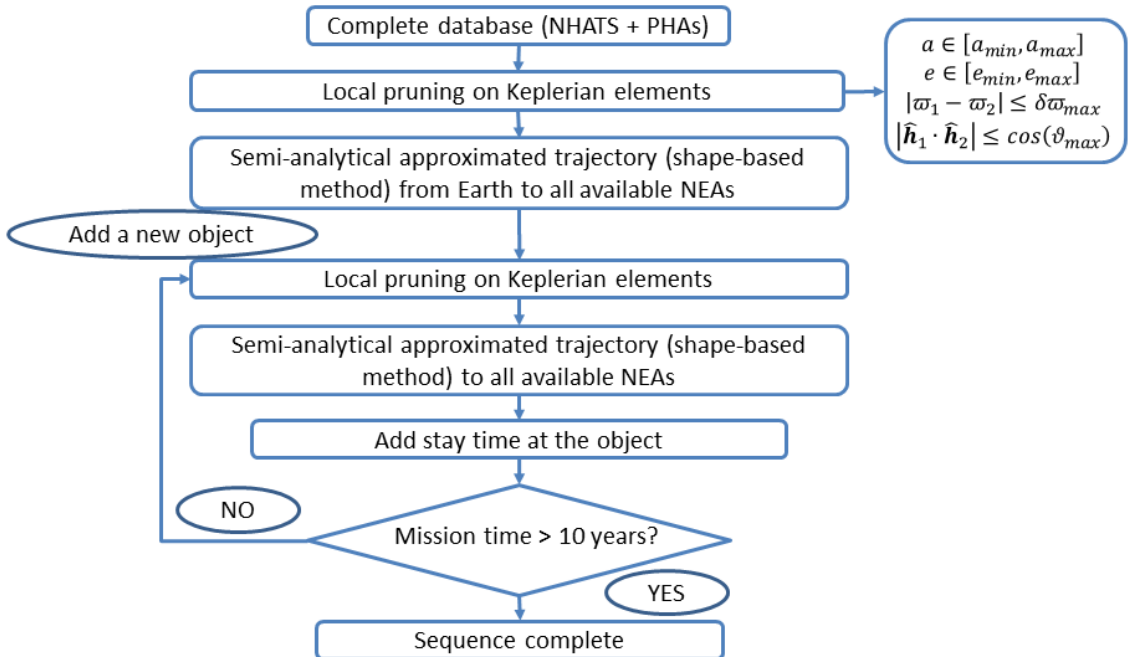


Fig. 3: Sequence search.



The sequence search described takes as more computational time as the number of feasible transfer trajectories increases, due to the tree nature of the search itself. For this reason, a mixed MATLAB/C code has been written to speed up the computation where bottle necks have been found in the MATLAB code. Moreover, the algorithm can work in parallel for different launch dates.

### 3.2.1. Simplified trajectory model: shape-based approach

Because no analytical solutions exist for solar sail trajectories, an optimization problem should be solved for each object tested. Furthermore, the number of trajectories to be tested within the sequence search is very large and solving an optimization problem for each of these trajectories results in an overall computational time to be too large. For this reason, the trajectory model used shall give results fast enough in order to have complete sequences in a reasonable amount of time. On the other hand, the solutions given by the trajectory model should be as closer to the real ones as possible, in order to have an overall trustworthiness on the sequences found. A possible simplified trajectory model can be found by using a Lambert-arc approximation, where the acceleration needed for the transfer is compared with the acceleration that the solar sail can provide. However, a low-thrust trajectory differs from the Lambert-arc approximation and this difference can be more marked for either very short or very long time of flight (ToF). Moreover, a solar sail is usually preferred for long ToF, because it can provide a high  $\Delta v$  without any limitation on the amount of propellant used. For this reason, a different simplified trajectory model, based on the shape of the trajectory, has been used in this study.

The core of the shape-based method is to find a set of analytic functions for each element in the state vector so that the shape of a low-thrust trajectory can be provided. In the two-body problem approximation, the acceleration  $\mathbf{a}$  needed to reach the designed trajectory is:

$$\mathbf{a} = \ddot{\mathbf{r}} + \mu \frac{\mathbf{r}}{r^3} \quad (6)$$

where  $\mathbf{r}$  is the position vector in Cartesian coordinates and  $\mu$  is the Sun's gravitational constant. So, once the shape of the trajectory is defined via a set of shaping functions, the control is analytically retrieved through Eq. (6) without any optimization needed. On the other hand, all the constraints on the acceleration achievable by the spacecraft can be only checked *a posteriori*. For this reason, some parameters (the shaping and the phasing parameters) are introduced in the set of shaping functions, so that one can tune them in order to find the trajectory which best fits the acceleration constraints.

As discussed in [7], a set of shaping functions for a coplanar transfer trajectory has been used. In order to avoid numerical issues, the state vector is expressed in terms of modified equinoctial elements [10]:

$$\mathbf{x} = [p \quad f \quad g \quad h \quad k \quad L]^T \quad (7)$$

where:

$$\begin{cases} p = a(1 - e^2) \\ f = e \cos(\omega + \Omega) \\ g = e \sin(\omega + \Omega) \\ h = \tan(i/2) \cos \Omega \\ k = \tan(i/2) \sin \Omega \\ L = \nu + \omega + \Omega \end{cases} \quad (8)$$

and  $\mathbf{x}^{kep} = [a, e, i, \Omega, \omega, \nu]^T$  is the set of the conventional Keplerian elements.

By considering the true longitude  $L$  as the independent variable, the set of shaping functions that describes the coplanar solar sail transfer trajectory is the following:

$$\begin{cases} p = p_0 \exp[p_1(L - L_0)] + \lambda_1 \sin(L - \phi_1) \\ f = f_0 + f_1(L - L_0) + \lambda_2 \sin(L - L_0 + \phi_2) \\ g = g_0 + g_1(L - L_0) - \lambda_2 \cos(L - L_0 + \phi_2) \end{cases} \quad (9)$$

where  $L_0$  is the value of the true longitude at the starting point,  $\{p_0, f_0, g_0\}$  and  $\{p_1, f_1, g_1\}$  depend on the initial and final condition, respectively. The terms  $\{\lambda_1, \lambda_2\}$  and  $\{\phi_1, \phi_2\}$  are the shaping and phasing parameters, respectively. These two set of parameters are those ones used to adjust the shape in order to find an acceleration history as close as possible to the one given by a solar sail (Eq. (2)). Because the shaping functions depend on the true longitude and  $\{p_1, f_1, g_1\}$  depend on the arrival point, but no mathematical relationship is used for the variation of the true longitude in time, a further constraint on the time of flight shall be checked, as discussed in De Pascale and Vasile [11].

A genetic algorithm is used for each trajectory computation test in order to check if a feasible solar sail trajectory exists by properly tuning the shaping and phasing parameters and the time of flight. Taking into account the heuristic nature of the genetic algorithm, a maximum of 3,000 generations is allowed, resetting the population up to three times in case of stalls.

### 3.2.2. Local pruning of the database

A local pruning on the whole available NEAs database is performed, on the basis of astrodynamical considerations: this has been carried out in order to work on a locally reduced database, for the reasons mentioned in Section 3.1. As shown in Fig. 3, the local pruning is performed at each leg of the sequence and it depends on the starting body of the leg, as explained below.

Four conditions for the local pruning of the database are taken into account: the first three criteria are related to the in-plane trajectory, while the fourth takes into account the out-of-plane orbit.

The four conditions for the local pruning of the database are as follows.

- i) The first local pruning is based on the semi-major axis change: the trajectory is propagated in an outward and inward spiral by considering a control law



which maximizes the semi-major axis change. The maximum and minimum semi-major axes obtained are, then, the range of semi-major axes that the solar sail can reach starting from the current state and traveling for the maximum available ToF. All those NEAs with a semi-major axis outside the available range are therefore excluded from the locally pruned database for the current leg.

In order to obtain the maximum and minimum semi-major axes, the locally-optimal solar sail trajectories described in [12] for a change of the in-plane Keplerian elements are taken into account. The optimal sail cone and clock angles can be expressed as:

$$\begin{cases} \alpha = \begin{cases} \alpha^* & \text{if } \alpha^* \leq \tan^{-1}(1/\sqrt{2}) \\ \tan^{-1}(1/\sqrt{2}) & \text{if } \alpha^* > \tan^{-1}(1/\sqrt{2}) \end{cases} \\ \delta = 0 \end{cases} \quad (10)$$

where

$$\tan \alpha^* = \frac{-3 + \sqrt{9 + 8 \tan^2 \tilde{\alpha}}}{4 \tan \tilde{\alpha}} \quad (11)$$

The angle  $\tilde{\alpha}$  in Eq. (11) represents the cone angle relative to the direction of the thrust for the maximization of the change of the desired orbital element. For the maximization of the semi-major axis, this angle is expressed as:

$$\tan \tilde{\alpha} = \frac{1 + e \cos \nu}{e \sin \nu} \quad (12)$$

- ii) The second local pruning is based on the eccentricity change. As in the previous case, the trajectory is propagated by considering a control law which maximizes the change of the eccentricity and thus a maximum range of possible eccentricity variation is found. Only those NEAs with eccentricity inside the available range are included in the locally pruned database for the current leg. As previously, the optimal sail cone and clock angles are given by Eqs. (10)-(11), but for this case the angle  $\tilde{\alpha}$  is given by the following relation:

$$\tan \tilde{\alpha} = \frac{2 + e \cos \nu}{1 + e \cos \nu} \cot \nu + \frac{e \operatorname{cosec} \nu}{1 + e \cos \nu} \quad (13)$$

- iii) The third local pruning is based on the longitude of pericenter  $\varpi = \omega + \Omega$ . A transfer trajectory between two orbits with a large  $\Delta \varpi = |\varpi_1 - \varpi_2|_\pi$  is, in fact, as more difficult as the eccentricities of the two orbits increase. This can be verified with the following test cases, where two 200 days transfers are computed by means of Lambert-arc approximation. Departing and arrival orbits are the same in both test cases, a part of the value of the eccentricity, as shown in Eqs. (14)-(15):

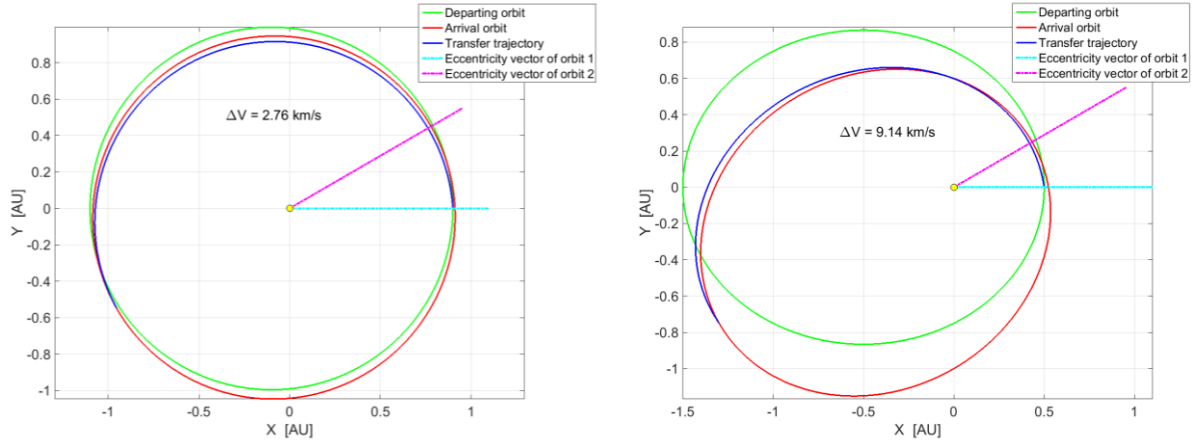
#### TEST CASE 1

$$\begin{cases} \mathbf{x}_{dep}^{kep} = [1 \text{ AU} & 0.1 & 0 & 0 & 0 & 0]^T \\ \mathbf{x}_{arr}^{kep} = [1 \text{ AU} & 0.1 & 0 & 30 \text{ deg} & 0 & 180 \text{ deg}]^T \end{cases} \quad (14)$$

## TEST CASE 2

$$\begin{cases} \mathbf{x}_{dep}^{kep} = [1 \text{ AU} & 0.5 & 0 & 0 & 0 & 0]^T \\ \mathbf{x}_{arr}^{kep} = [1 \text{ AU} & 0.5 & 0 & 30 \text{ deg} & 0 & 180 \text{ deg}]^T \end{cases} \quad (15)$$

Fig. 4 shows the single-revolution Lambert-arc solution of both the transfer trajectories. The difference in the required  $\Delta v$  is highlighted in the figure. It can be seen how the required  $\Delta v$  in the second test case is more than 3 times greater than the one needed in the first case.



a)

b)

Fig. 4: Heliocentric view of the transfer trajectory. a) test case 1. b) test case 2.

For the reason described above, a threshold on the maximum variation of the longitude of pericenter has been considered for each object, taking into account the value of the eccentricity as follows:

$$\delta\varpi_{\max} := \pi(1-e)^2 \quad (16)$$

By using this threshold, the arrival object is removed from the locally pruned database if at least one of the following conditions is not satisfied:

$$\begin{cases} \left| \varpi_1 + \delta\varpi_{\max,1} + \pi \right|_{2\pi} > \left| \varpi_2 - \delta\varpi_{\max,2} + \pi \right|_{2\pi} \\ \left| \varpi_2 + \delta\varpi_{\max,2} + \pi \right|_{2\pi} > \left| \varpi_1 - \delta\varpi_{\max,1} + \pi \right|_{2\pi} \end{cases} \quad (17)$$

In Fig. 5, two examples (not to scale) are sketched in order to give a graphical view of the pruning on the longitude of pericenter given by Eq. (17). Fig. 5a shows a case in which Eq. (17) is satisfied and, in fact, the ranges of possible variation of  $\varpi$  for the two objects overlap. On the other hand, in Fig. 5b the orbit of the second object is more eccentric, so that the available range of variation of  $\varpi$  is smaller and it does not overlap with the one of the first object. In this second case, the first condition in Eq. (17) is not satisfied and the second object is, therefore, not part of the locally pruned database for the current leg.

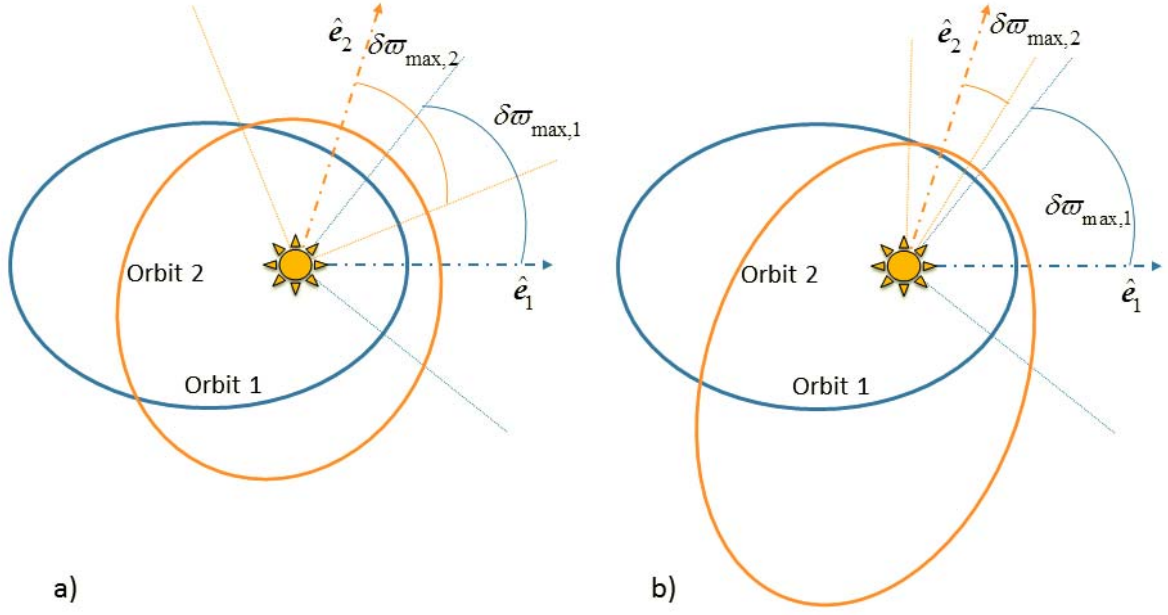


Fig. 5: Graphical view (not to scale) of the pruning on the longitude of pericenter. a) a case in which the ranges of possible variation of  $\varpi$  for the two objects overlap; b) a case in which the ranges of possible variation of  $\varpi$  for the two objects do not overlap.

- iv) The last condition considers the angular momentum of the orbit. Let us define  $\mathcal{J}$  as the angle between the angular momenta of the two orbits:

$$\mathcal{J} = \arccos \left| \hat{\mathbf{h}}_1 \cdot \hat{\mathbf{h}}_2 \right| \quad (18)$$

Because a coplanar transfer is taken into account for the simplified trajectory description, a maximum value of  $\mathcal{J}$  is selected as threshold in order to consider the second object to be part or not of the locally pruned database.

#### 4. Sequence optimization

Once complete sequences have been found via the sequence search algorithm described in Section 3, an optimization problem must be solved in order to find 3D solar sail trajectories.

The equations of the dynamics are defined by the following set of ordinary differential equations of motion [13]:

$$\dot{\mathbf{x}}(t) = \mathbf{A}(\mathbf{x})\mathbf{a} + \mathbf{b} \quad (19)$$

where  $\mathbf{A}$  is the matrix of the dynamics expressed, in the orbital reference frame  $\{\hat{\mathbf{r}}, \hat{\boldsymbol{\theta}}, \hat{\mathbf{h}}\}$ , as:

$$\mathbf{A} = \begin{bmatrix} 0 & \frac{2p}{q} \sqrt{\frac{p}{\mu}} & 0 \\ \sqrt{\frac{p}{\mu}} \sin L & \sqrt{\frac{p}{\mu}} \frac{1}{q} \{(q+1) \cos L + f\} & -\sqrt{\frac{p}{\mu}} \frac{g}{q} \{h \sin L - k \cos L\} \\ -\sqrt{\frac{p}{\mu}} \cos L & \sqrt{\frac{p}{\mu}} \frac{1}{q} \{(q+1) \sin L + g\} & \sqrt{\frac{p}{\mu}} \frac{f}{q} \{h \sin L - k \cos L\} \\ 0 & 0 & \sqrt{\frac{p}{\mu}} \frac{s^2 \cos L}{2q} \\ 0 & 0 & \sqrt{\frac{p}{\mu}} \frac{s^2 \sin L}{2q} \\ 0 & 0 & \sqrt{\frac{p}{\mu}} \frac{1}{q} \{h \sin L - k \cos L\} \end{bmatrix} \quad (20)$$

$\mathbf{b}$  is:

$$\mathbf{b} = \begin{bmatrix} 0 & 0 & 0 & 0 & 0 & \sqrt{\mu p} \left( \frac{q}{p} \right)^2 \end{bmatrix}^T \quad (21)$$

and the propulsive acceleration  $\mathbf{a}$  is given by Eq. (2). The terms  $q$  and  $s^2$  that appear in Eqs. (20)-(21) are auxiliary variables, defined as:

$$\begin{aligned} q &= 1 + f \cos L + g \sin L \\ s^2 &= 1 + h^2 + k^2 \end{aligned} \quad (22)$$

The problem of finding the optimal control vector  $\mathbf{u} = [N_r^* \quad N_g^* \quad N_h^*]^T$ , such that the total mission duration is minimized while fulfilling the dynamics constraints of Eq. (19) at any time, is solved via a direct transcription method [14]. The trajectory found through the coplanar shape-based approach is used as a first guess solution for the optimizer, which transforms it into a complete 3D trajectory.

It is worth to note that at this stage of the work an optimal solution is not strictly required. Because an approximated model for the trajectory description has been used in the sequence search, the aim of this optimization phase is mainly to check the reliability of the sequence search algorithm (i.e. check that the sequences found in the tree search algorithm are actually feasible by the given solar sail). For this reason, although an optimal solution is preferred, a solution which satisfies all the constraints on time, state and control, but not the optimality conditions, is considered good enough.

An algorithm has been developed in MATLAB to find the optimal trajectory in terms of total mission duration (Fig. 6). Given the selected sequence, the algorithm:

- 1) Automatically computes the initial guess for each leg separately
- 2) Optimizes the 3D trajectory leg by leg with several sets of optimization parameters (e.g. with or without an internal scaling method)
- 3) Finally, if a feasible trajectory is found in all the legs individually, the whole multi-leg trajectory is optimized all-at-once.

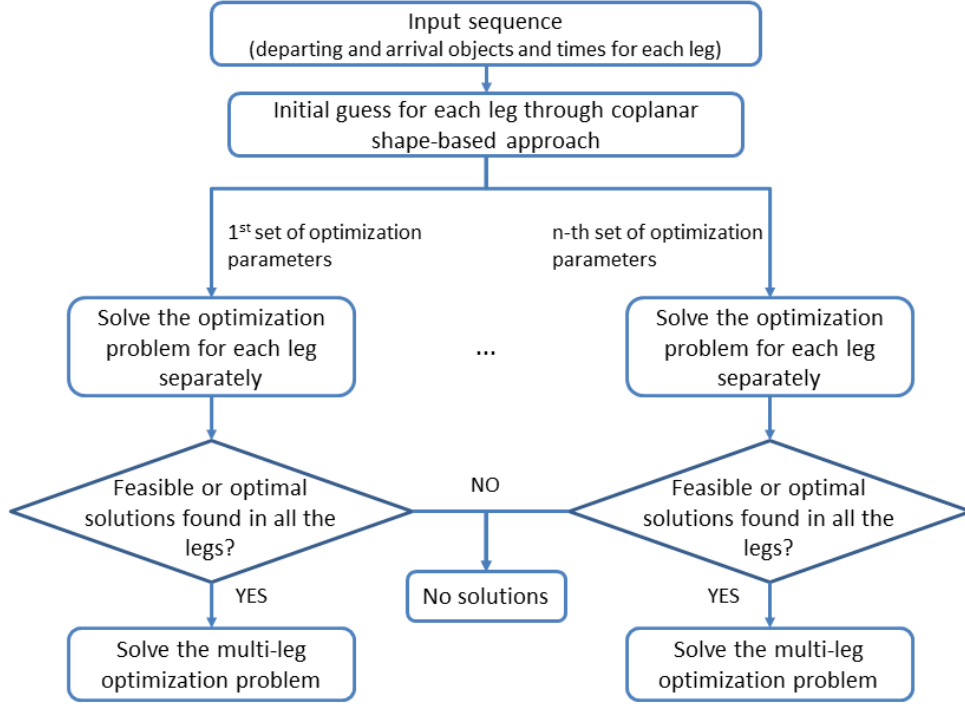


Fig. 6: Automatic optimization algorithm.

## 5. Problem description

The reference work of Dachwald et al. [8] showed a 3-NEA rendezvous mission through solar sailing, considering a sailcraft with a characteristic acceleration  $a_c = 0.3 \text{ mm/s}^2$ . The sequence of encounters, according to the DLR/ESA Gossamer roadmap to solar sailing [8], should respect the following criteria:

- At least one object should be a PHA.
- At least one object should be a potential target for future human exploration (i.e. should be part of the temporary NHATS database).
- The last NEA should be a very small object (i.e.  $H \geq 25.5 \text{ mag}$ ).

Because of the nature of the sequence search method described in Section 3, these criteria can only be verified *a posteriori*. Although no guarantees are given about meeting the requirements above, a large number of sequences are discovered. Therefore, the candidate sequences are chosen as those ones that best fit criteria a) - c) and that are made of the largest number of encounters.

Moreover, Dachwald et al. [8] proposed three further steps to be investigated in future works:

- Reduction of total mission duration.
- Reduction of required characteristic acceleration.
- Priority on PHA within target selection.

A reduction in the total mission duration has not been taken into account in the current work, but sequences with more than 3 objects have been found, as presented in Section 6.1.

A reduction of the required characteristic acceleration with respect to the one used in the Gossamer study ( $a_c = 0.3 \text{ mm/s}^2$ ) was addressed by considering a solar sail with a characteristic acceleration  $a_c = 0.2 \text{ mm/s}^2$ . This means, according to Eq. (3),

a reduction of the area-to-mass ratio from  $A/m|_{a_c=0.3} = 33 \text{ m}^2/\text{kg}$  to  $A/m|_{a_c=0.2} = 22 \text{ m}^2/\text{kg}$ . The latter implies the possibility of either carrying more payload on the same sailcraft, or using a smaller sail or a heavier structure, with the result of raising the TRL. According to the DLR/ESA Gossamer technology [9], such a reduction in the characteristic acceleration implies reducing the sail size from about  $(54 \text{ m})^2 - (65 \text{ m})^2$  to about  $(39 \text{ m})^2 - (48 \text{ m})^2$ . The interval of sail dimensions depends on the sailcraft bus adopted, as discussed in [8].

Finally, only PHAs and NHATS asteroids have been considered in the whole database of objects for the sequence search and the solutions with at least one PHA are preferred to the others.

## 6. Results

In the following subsections the results of the sequence search and some fully optimized sequences are shown.

### 6.1. Sequence search results

Starting from the departing date of the reference mission (i.e.  $t_0 = 28 \text{ Nov } 2019$ ), a systematic search of sequences has been carried out on a set of launch dates spanning 10 years with a step size of 3 months ( $t_0 \in [28 \text{ Nov } 2019, 06 \text{ Oct } 2029]$ ). This choice of the launch dates allows taking into account short and long term variations in the phasing between the objects.

This search resulted in more than 1,000 unique sequences made of 5 encounters, of which one is a PHA. It is important to underline that all the sequences found in the current work contain only NHATS asteroids and sometimes also a PHA.

Due to the tree nature of the sequence search and the need of a genetic algorithm run to check the existence of each trajectory, the whole search has been carried out by running several parallel searches for 40 different launch dates over two machines: a 3.4 GHz Core i7-3770 and a 3.4 GHz Core i7-2600 both with 16 GB of RAM and running Windows 7. The hyper-threading was disabled in the first machine, such that no virtual cores are present and each core performs at the maximum level. The average computational time for each sequence search run on the first machine is about 6 days, while on the second one is about 17 days. Because on the second machine the hyper-threading was enable, up to 8 sequence search runs in parallel could be performed there, but each run could have access to about half of the total available core performance.

Fig. 7 shows the number of unique 5-NEA sequences found along the different launch dates tested. Only those sequences with one PHA are taken into account for the plot, but the total number of unique sequences with 5 encounters is even greater (689 unique sequences with 5 encounters have been found for the launch date  $t_0 = 14 \text{ Apr } 2028$ ). Up to 400 unique sequences with one PHA have been found for a single launch date ( $t_0 = 09 \text{ Jan } 2029$ ) by taking into account only those sequences with 4 encounters and even more if we consider only 3-NEAs rendezvous.

However, we are aware that a coding issue over-constrained the pruning on eccentricity. For this reason, we expect that the actual number of sequences is even larger.



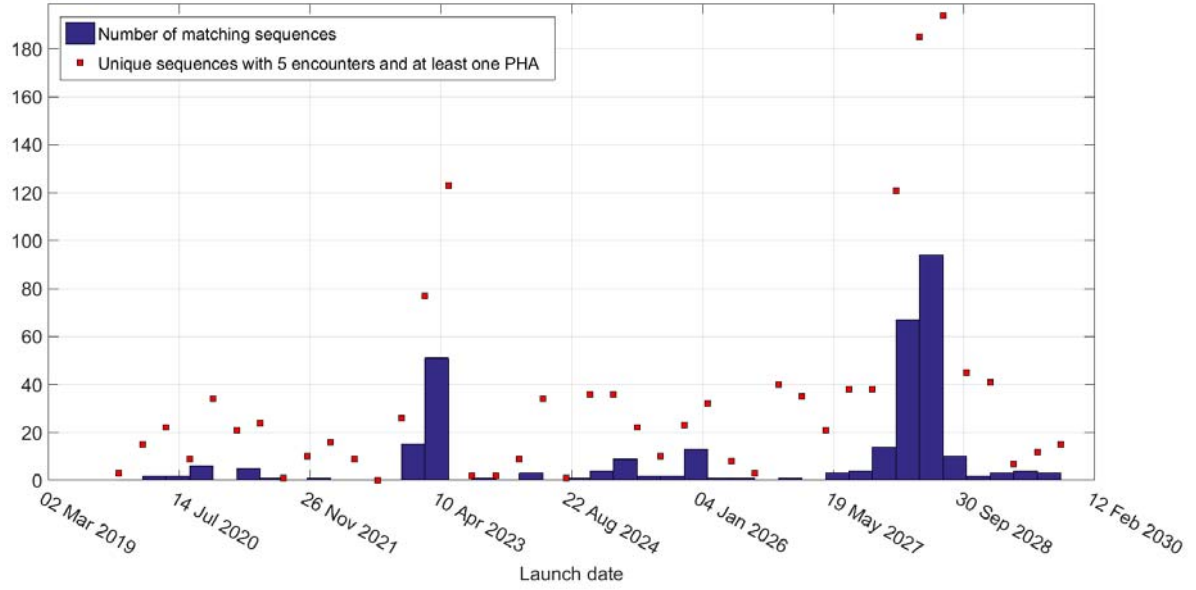


Fig. 7: Number of unique sequences with 5 NEAs and one PHA as a function of the launching date. The blue bars show the number of matching sequences between two consecutive departing dates.

## 6.2. Sequence optimization results

Two sequences have been selected as samples, and fully optimized by means of the automatic algorithm described in Section 4, in order to validate the methodology proposed. These sequences have been selected among all the sequences found with 5 encounters, of which one is a PHA and the last object is small, as from the mission requirements a) - c) in Section 5.

Table 2 and Table 3 show the characteristics of the encounters in the sequences studied. Note that the change in inclination between two consecutive objects is always less than 5 deg, which is the threshold used for the coplanar approximation (Eq. **Error! Reference source not found.**).

SEQUENCE 1	2014 EK <sub>24</sub>	2013 PA <sub>7</sub>	2012 MD <sub>7</sub>	2000 EA <sub>14</sub>	2008 DB
Orbital type	Apollo	Amor	Aten	Apollo	Apollo
Semi-major axis [AU]	1.004	1.154	0.977	1.117	1.055
Eccentricity	0.072	0.087	0.109	0.202	0.233
Inclination [deg]	4.722	3.474	3.754	3.555	4.223
Absolute magnitude [mag]	23.2	22.6	24.1	21.1	25.7
Estimated size [m]	65 – 150	85 – 190	40 – 95	170 – 370	20 – 50
EMOID [AU]	0.034	0.091	0.018	0.043	0.002
PHA	no	no	no	yes	no
NHATS	yes	yes	yes	no	yes

Table 2: Properties of the encounters of sequence 1.

SEQUENCE 2	2008 BT <sub>2</sub>	2013 EM <sub>89</sub>	2005 TG <sub>50</sub>	2011 CG <sub>2</sub>	2011 UX <sub>275</sub>
Orbital type	Amor	Amor	Aten	Apollo	Apollo
Semi-major axis [AU]	1.173	1.178	0.923	1.177	1.035
Eccentricity	0.081	0.117	0.134	0.158	0.076
Inclination [deg]	3.075	2.411	2.401	2.757	4.541
Absolute magnitude [mag]	24.3	26.0	24.8	21.5	25.8
Estimated size [m]	35 – 75	17 – 37	25 – 60	130 – 300	17 – 37
EMOID [AU]	0.087	0.044	0.013	0.031	0.018
PHA	no	no	no	yes	no
NHATS	yes	yes	yes	yes	yes

Table 3. Properties of the encounters of sequence 2.

By following the optimization steps described in Fig. 6, a multi-leg optimal solution has been found for both the sequences studied. The main characteristics of the missions are briefly listed in Table 4 and Table 5.







Object	Stay time [days]		Start	End	ToF [days]
Earth	//		07/12/2021	15/10/2023	678
2014 EK <sub>24</sub>	104		27/01/2024	17/03/2025	414
2013 PA <sub>7</sub>	183		15/09/2025	08/08/2027	691
2012 MD <sub>7</sub>	113		29/11/2027	30/08/2029	640
2000 EA <sub>14</sub>	95		03/12/2029	26/04/2031	510
2008 DB	//				

Table 4: Mission parameters for sequence 1.







Object	Stay time [days]		Start	End	ToF [days]
Earth	//		04/02/2026	04/12/2027	668
2008 BT <sub>2</sub>	84		26/02/2028	01/05/2029	430
2013 EM <sub>89</sub>	175		23/10/2029	07/07/2031	622
2005 TG <sub>50</sub>	63		08/09/2031	26/05/2033	627
2011 CG <sub>2</sub>	99		03/09/2033	29/06/2035	664
2011 UX <sub>275</sub>	//				

Table 5: Mission parameters for sequence 2.

For both the missions shown, the sailcraft is injected directly into an interplanetary trajectory at Earth, with characteristic energy  $C_3 = 0 \text{ km}^2/\text{s}^2$ , and completes its mission in about 9.4 years. It is worth noting that the sailcraft spends at least 2 months in the proximity of each object, giving the possibility of close-up NEA observations for a considerable amount of time.

The complete trajectory of the first sequence is shown in Fig. 8.

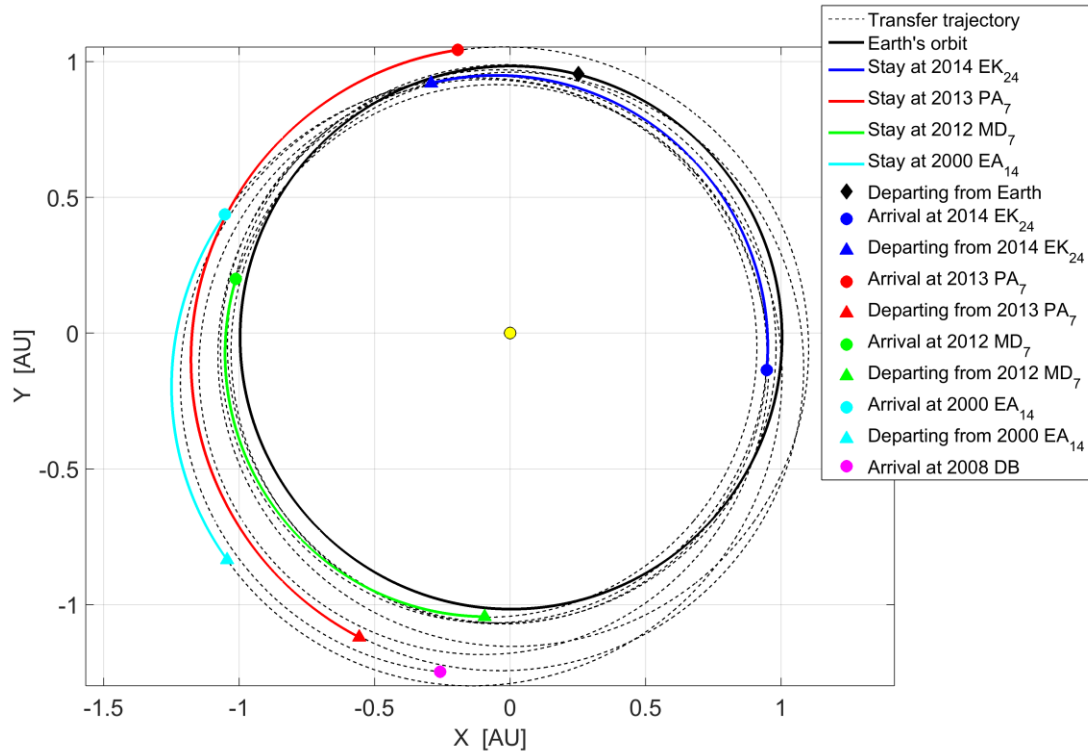


Fig. 8: Heliocentric view of the complete three-dimensional trajectory of sequence 1.

In Fig. 9 the transfer trajectories for each leg are shown, where the dotted black line represents the orbit of the Earth, the green line is the orbit of the departing object, the red line the orbit of the arrival one and the blue line is the transfer trajectory.

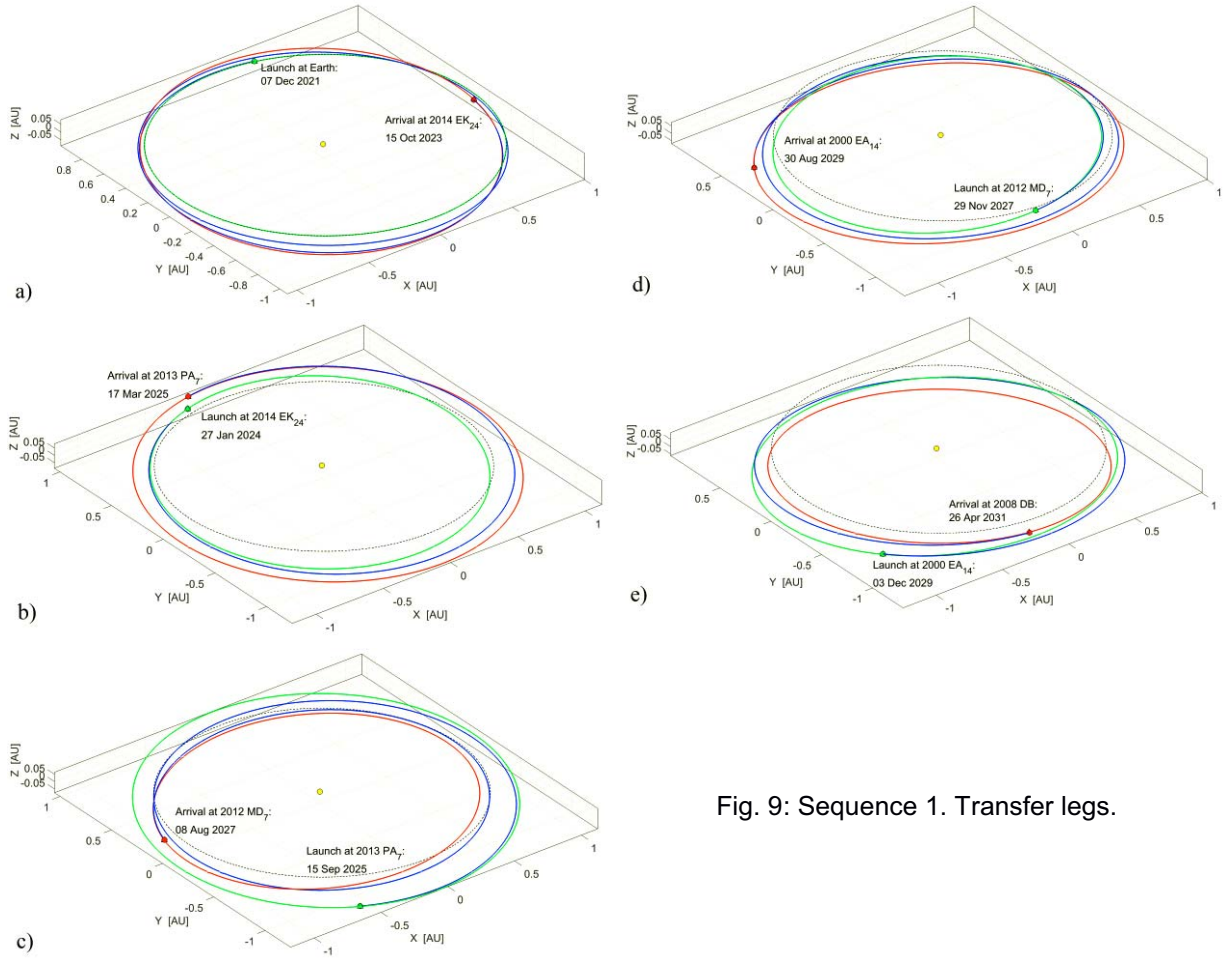


Fig. 9: Sequence 1. Transfer legs.

Fig. 10 shows the trend of cone and clock angles over time for the first sequence.

It is worth noting that, despite of the few spikes in the control angles shown in Fig. 10, the results are completely feasible by a traditional, non-high performing, solar sail: for example, for the spike in the clock angle that occurs at  $ToF \approx 220$  days (Fig. 10b) a maneuver of  $\delta \approx 143$  deg in 15 days is required. Studies on solar sail attitude control in literature show that a solar sail with a characteristic acceleration  $a_c < 0.1 \text{ mm/s}^2$  is able to perform a 35 deg maneuver in about 4 hours [15].

However, a further optimization with a more precise method can help to smooth out the control history.

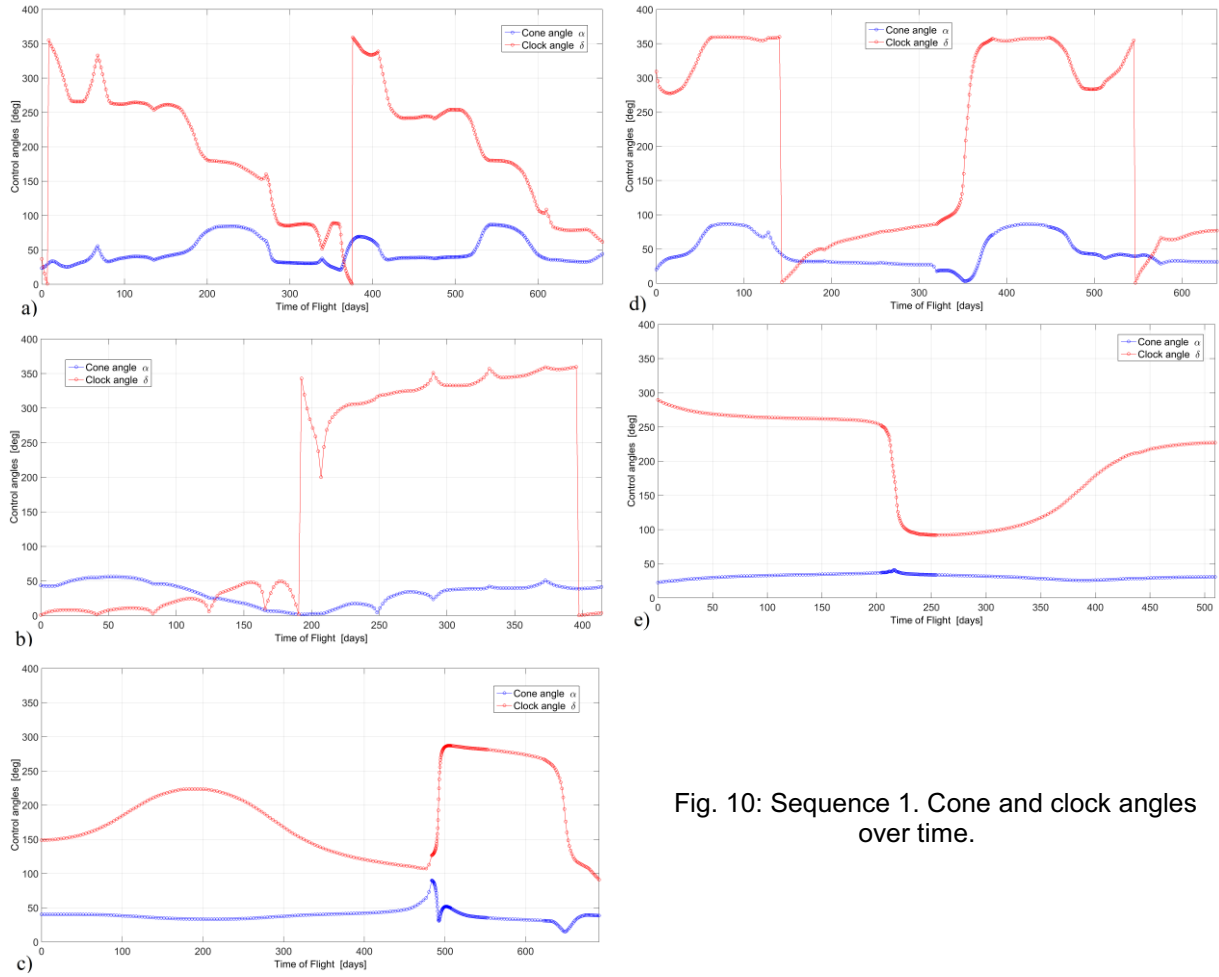


Fig. 10: Sequence 1. Cone and clock angles over time.

## 7. Conclusions

A methodology to find sequences of encounters for multiple Near-Earth Asteroids (NEAs) rendezvous mission through solar sailing was presented. In order to increase the possibility of finding objects of interest for both a planetary defense and a scientific point of view, only Potentially Hazardous Asteroids (PHAs) and Near-Earth Object Human Space Flight Accessible Target Study (NHATS) asteroids were pre-selected to being part of the database under study. Apart of the certainty of selecting objects of some interest, this allowed a reduction in the total computational effort needed in finding sequences. Local pruning, based on astrodynamical criteria, has been used in order to find as many sequences as possible with a reduced amount of computational time. Therefore, a simplified shape-based solar sail trajectory model was taken into account in order to have a good approximation of the trajectory, ensuring that the sequence is likely to be feasible with a detailed trajectory model. Finally, an automatic algorithm was developed in order to optimize the full solar sail trajectory of the sequences chosen from the output of the sequence search.

A wide range of launch dates has been tested. This has been done in order to have more flexibility on the initial mission time and the possibility to choose a launch window also on the basis of the amount of possible sequences.

Some test sequences have been fully optimized for the complete multi-leg trajectory, resulting in total mission durations less than 10 years and at least 2 months spent in the vicinity of each object for close-up observations.

This work resulted in more than 1,000 unique sequences made of 4 NHATS asteroids and a PHA within less than 10 years of total mission duration. Furthermore, a solar sail with a reduced performance than the one considered in the reference study has been taken into account in this work. This means a step further in the Gossamer roadmap to solar sailing, as a lower characteristic acceleration implies a smaller or less-lightweight sail for the same spacecraft bus. As a consequence, this study can increase the Technology Readiness Level of this kind of mission.

Future work will focus on reducing the computational time required by the sequence search, as well as on the study of a 3D approximation of the solar sail trajectory, in order to have more reliable sequences from the sequence search.

## References

- [1] Boden, R. C., Hein, A. M. and Kawaguchi, J., "Target selection and mass estimation for manned NEO exploration using a baseline mission design", *Acta Astronautica*, (2015, In Press).
- [2] Korsmeyer, D. J., Landis, R. R. and Abell, P. A., "Into the beyond: A crewed mission to a near-Earth object", *Acta Astronautica*, Vol. 63, No. 1–4, 2008, pp. 213-220.
- [3] Sanchez, P., Colombo, C., Vasile, M. and Radice, G., "Multicriteria Comparison Among Several Mitigation Strategies for Dangerous Near-Earth Objects", *Journal of Guidance, Control, and Dynamics*, Vol. 32, No. 1, 2009, pp. 121-142.
- [4] Sugimoto, Y., Radice, G. and Sanchez, J. P., "Effects of NEO composition on deflection methodologies", *Acta Astronautica*, Vol. 90, No. 1, 2013, pp. 14-21.
- [5] "NEOShield: A Global Approach to Near-Earth Object Impact Threat Mitigation", 2012, <http://www.neoshield.net/en/index.htm>.
- [6] Mainzer, A., Grav, T., Masiero, J., Bauer, J., McMillan, R. S., Giorgini, J., Spahr, T., Cutri, R. M., Tholen, D. J., Jedicke, R., Walker, R., Wright, E. and Nugent, C. R., "Characterizing Subpopulations within the near-Earth Objects with NEOWISE: Preliminary Results", *The Astrophysical Journal*, Vol. 752, No. 2, 2012.
- [7] Peloni, A., Ceriotti, M. and Dachwald, B., "Preliminary Trajectory Design of a Multiple NEO Rendezvous Mission Through Solar Sailing", *65th International Astronautical Congress*, International Astronautical Federation, Toronto, Canada, 2014.
- [8] Dachwald, B., Boehnhardt, H., Broj, U., Geppert, U. R. M. E., Grundmann, J.-T., Seboldt, W., Seefeldt, P., Spietz, P., Johnson, L., Kührt, E., Mottola, S., Macdonald, M., McInnes, C. R., Vasile, M. and Reinhard, R., "Gossamer Roadmap Technology Reference Study for a Multiple NEO Rendezvous Mission," *Advances in Solar Sailing*, edited by M. Macdonald, Springer Praxis Books, Springer Berlin Heidelberg, 2014, pp. 211-226.
- [9] Geppert, U. R. M. E., Biering, B., Lura, F., Block, J., Straubel, M. and Reinhard, R., "The 3-step DLR-ESA Gossamer road to solar sailing", *Advances in Space Research*, Vol. 48, No. 11, 2011, pp. 1695-1701.
- [10] Walker, M. J. H., Ireland, B. and Owens, J., "A set modified equinoctial orbit elements", *Celestial mechanics*, Vol. 36, No. 4, 1985, pp. 409-419.



- [11] De Pascale, P. and Vasile, M., "Preliminary design of low-thrust multiple gravity-assist trajectories", *Journal of Spacecraft and Rockets*, Vol. 43, No. 5, 2006, pp. 1065-1076.
- [12] McInnes, C. R., *Solar Sailing: Technology, Dynamics and Mission Applications*, Springer Praxis Publishing, Chichester, U.K., 1999.
- [13] Betts, J. T., *Practical Methods for Optimal Control and Estimation Using Nonlinear Programming*, Society for Industrial and Applied Mathematics (SIAM, 3600 Market Street, Floor 6, Philadelphia, PA 19104), 2010.
- [14] Patterson, M. A. and Rao, A. V., "GPOPS – II: A MATLAB Software for Solving Multiple-Phase Optimal Control Problems Using hp-Adaptive Gaussian Quadrature Collocation Methods and Sparse Nonlinear Programming", *ACM Transactions on Mathematical Software*, Vol. 39, No. 3, 2013.
- [15] Wie, B. and Murphy, D., "Solar-Sail Attitude Control Design for a Sail Flight Validation Mission", *Journal of Spacecraft and Rockets*, Vol. 44, No. 4, 2007, pp. 809-821.